# J|A|C|S

## A R T I C L E S

# Oxoclusters of the Lanthanides Begin to Resemble Solid-State Materials at Very Small Cluster Sizes: Structure and NIR Emission from Nd(III)

Santanu Banerjee,[†] G. Ajith Kumar,[‡] Richard. E. Riman,[‡] Thomas J. Emge,[†] and John G. Brennan*,[†]

*Contribution from the Department of Chemistry and Chemical Biology, Department of Materials Science and Engineering, Rutgers, the State University of New Jersey, 610 Taylor Road, Piscataway, New Jersey 08854-8087*

Received December 15, 2006; E-mail: bren@ccbmail.rutgers.edu

**Abstract:** The reaction of $Nd(SePh)_3$ with $SeO_2$ and Hg in pyridine gives the dodecanuclear cluster $[(py)_{18}Nd_{12}O_6Se_4(Se_2)_4(SePh)_4(Se_2Ph)_2Hg_2(SePh)_4][(Hg(SePh)_3]_2$. In this compound the 12 Nd(III) ions are stacked in four sets of $Nd_3$, with pairs of tetrahedral oxo ligands separating the $Nd_3$ planes and Se, SeSe, SePh, pyridine, and HgSePh groups encapsulating the oxo core. Both the Nd−O bond lengths and the geometries about the oxo ions are remarkably similar to those found in solid-state $Nd_2O_3$. Near-IR emission experiments indicate that the cluster emission properties are less intense than those of highly emissive $(DME)_2Nd(SC_6F_5)_3$ or $(THF)_8Nd_8O_2Se_2(SePh)_{16}$ but brighter than the nonemissive solid-state compound $Nd_2O_3$. Intensity variations are interpreted in terms of concentration quenching and phonon relaxation.

## Introduction

Emission of light from lanthanide ions is a fundamentally important process with a continuously expanding range of applications in contemporary electronic devices, from TV screens to lasers and optical fibers.[1−5] Control of emission intensity is often elusive, with competitive processes such as upconversion, down-conversion, cross-relaxation, photon splitting, or nonradiative (vibronic) quenching often detracting from ideal performance.[6] While introduction of Ln into solid-state oxide materials has long been facile, the incorporation of near-IR emissive lanthanide ions into emerging materials (i.e., organic polymers) remains challenging[7−16] due to the intrinsic properties of Ln sources and the various technological barriers associated with solids processing.

Lanthanide cluster compounds, with their solubility in organic solvents and their relatively high concentration of Ln ions/unit volume, are promising sources of lanthanide ions in the preparation of emissive composite materials. These clusters can be quite emissive, if ligands with high-energy vibrational modes are excluded. For example, recent reports outlined the synthesis, characterization, and extraordinary properties of $Er^{17−20}$ and $Nd^{21}$ chalcogenido clusters. First noted was the 1.54 $\mu m$ emission with 78% quantum efficiency from $(THF)_{14}Er_{10}S_6$-$(SeSe)_6I_6$, and this was followed by the neodymium cluster $(THF)_8NdO_2Se_2(SePh)_{16}$ (Nd8), which showed emission at 1349 and 1832 nm, the latter wavelength being unprecedented for a molecular Nd source.

The Nd cluster was important not only because of the startling emission but also because the synthesis route was potentially general for the synthesis of increasingly large clusters. Further, the approach precluded the incorporation of fluorescence quenching OH ligands. While oxo chemistry of the lanthanides

† Department of Chemistry and Chemical Biology.
‡ Department of Materials Science and Engineering.

(1) Silversmith, A. J.; Lenth, W.; Macfarlane, R. M. *Appl. Phys. Lett.* **1987**, *51*, 1997.
(2) Maciel, G. S.; de Arajuo, C. B.; Massaddeq, Y.; Aegerter, M. A. *Phys. Rev. B* **1997**, *55*, 6335.
(3) Hebert, T.; Wannermacher, R.; Lenth, W.; Macfarlane, R. M. *Appl. Phys. Lett.* **1990**, *57*, 1727.
(4) Dowing, E.; Hesselink, L.; Ralston, J.; Macfarlane, R. M. *Science* **1986**, *273*, 1185.
(5) Bhargava, R. N.; Gallaghar, D.; Hong, X.; Nurmikko, A. *Phys. Rev Lett.* **1994**, 416.
(6) *Spectroscopy of Solid State Laser Type Materials*; Di Bartolo, B., Ed.; Plenum Press: New York, 1987.
(7) Hasegawa, Y.; Sogabe, K.; Wada, Y.; Yanagida, S. *J. Lumin.* **2003**, *101*, 235.
(8) Le Quang, A. Q.; Zyss, J.; Ledoux, I.; Truong, V. G.; Jurdyc, A. M.; Jacquier, B.; Le, D. H.; Gibaud, A. *Chem. Phys.* **2005**, *318*, 33.
(9) O'Riordan, A.; O'Connor, E.; Moynihan, S.; Llinares, X.; Van Deun, R.; Fias, P.; Nockemann, P.; Binnemans, K.; Redmond, G. *Thin Solid Films* **2005**, *491*, 264.
(10) Nichkova, M.; Dosev, D.; Gee, S. J.; Hammock, B. D.; Kennedy, I. M. *Anal. Chem.* **2005**, *77*, 6864.
(11) Wang, Z.; Samuel, I. D. W. *J. Lumin.* **2005**, *111*, 199.
(12) Bermudez, V.; Ostrovskii, D.; Lavoryk, S.; Goncalves, M. C.; Carlos, L. D. *Phys. Chem. Chem. Phys.* **2004**, *6*, 649.
(13) Binnemans, K.; Lenaerts, P.; Driesen, K.; Goerller-Walrand, C. *J. Mater. Chem.* **2004**, *14*, 191.
(14) de Souza, J. M.; Alves, S.; De Sa, S. F.; de Azevedo, W. M. *J. Alloys Cmpd.* **2002**, *344*, 320.
(15) Harrison, B. S.; Foley, T. J.; Knefely, A. S.; Mwaura, J. K.; Cunningham, G. B.; Kang, T.; Bouguettaya, M.; Boncella, J. M.; Reynolds, J. R.; Schanze, K. S. *Chem. Mater.* **2004**, *16*, 2938.
(16) Kang, T.; Harrison, B. S.; Foley, T. J.; Knefely, A. S.; Boncella, J. M.; Reynolds, J. R.; Schanze, K. S. *Adv. Mater.* **2003**, *15*, 1093.
(17) Kornienko, A.; Kumar, G. A.; Riman, R. E.; Emge, T. J.; Brennan, J. G. *J. Am. Chem. Soc.* **2005**, *127*, 3501.
(18) Kumar, G. A.; Kornienko, A.; Banerjee, S.; Riman, R. E.; Emge, T. J.; Brennan, J. G. *Chem. Mater.* **2005**, *17*, 5130.
(19) Kumar, G. A.; Riman, R. E.; Chen, S.; Smith, D.; Ballato, J.; Banerjee, S.; Kornienko, A.; Brennan, J. G. *Appl. Phys. Lett.* **2006**, *88*, 91902.
(20) Kornienko, A.; Banerjee, S.; Kumar, G. A.; Riman, R. E.; Emge, T. J.; Brennan, J. G. *J. Am. Chem. Soc.* **2005**, *127*, 14008.
(21) Banerjee, S.; Huebner, L.; Romanelli, M. D.; Kumar, G. A.; Riman, R. E.; Emge, T. J.; Brennan, J. G. *J. Am. Chem. Soc.* **2005**, *127*, 15900.

has, in the past, revealed a series of structures ranging from bimetallic molecules with Ln−O−Ln connectivities[22−26] to increasingly large (Ln 8, 9) oxo based clusters,[27−64] the tendency of these materials to include OH ligands has quenched interest in their emission properties.

Outlined here is the first clear examination of how dimensionality influences physical properties in lanthanide cluster compounds, in terms of both vibronic coupling and concentration quenching. The synthesis and characterization of the largest Ln hydroxy-free oxo cluster compound reported to date are described, the fluorescence properties of the compound are examined, and analogies to the properties of both molecular and solid-state materials are clearly defined.

(22) Adam, M.; Massarweh, G.; Fischer, R. D. *J. Organomet. Chem.* **1991**, *405*, C33.
(23) Dubé, T.; Gambarotta, S.; Yap, G. P. A. *Organometallics* **1998**, *17*, 3967.
(24) Zhang, X.; Loppnow, G. R.; McDonald, R.; Takats, J. *J. Am. Chem. Soc.* **1995**, *117*, 7828.
(25) Deelman, B. J.; Booij, M.; Meetsma, A.; Teuben, J. H.; Kooijman, H.; Spekt, A. L. *Organometallics* **1995**, *14*, 2306.
(26) Evans, W. J.; Grate, J. W.; Bloom, I.; Hunter, W. E.; Atwood, J. L. *J. Am. Chem. Soc.* **1985**, *107*, 405.
(27) Zalkin, A.; Berg, D. J. *Acta. Crystallogr.* **1989**, *CA5*, 1630.
(28) Zhou, X.; Ma, H.; Wu, Z.; You, X.; Xu, Z.; Huang, X. *J. Organomet. Chem.* **1995**, *503*, 11.
(29) Pernin, C. G.; Ibers, J. A. *Inorg. Chem.* **1997**, *36*, 3802.
(30) Anwander, R.; Munck, F. C.; Priermeier, T.; Scherer, W.; Runte, O.; Herrmann, W. A. *Inorg. Chem.* **1997**, *36*, 3545.
(31) Evans, W. J.; Sollberger, M. S.; Hanusa, T. P. *J. Am. Chem. Soc.* **1988**, *110*, 1841.
(32) Yunlu, K.; Gradeff, P. S.; Edelstein, N.; Kot, W.; Shalimoff, G.; Streib, W. E.; Vaartstra, B. A.; Caulton, K. G. *Inorg. Chem.* **1991**, *30*, 2317.
(33) Liu, J.; Meyers, E. A.; Shore, S. G. *Inorg. Chem.* **1998**, *37*, 5410.
(34) Giester, G.; Unfried, P.; Zyak, Z. *J. Alloys Cmpd.* **1997**, *257*, 175.
(35) Wang, R.; Zheng, Z.; Jin, T.; Staples, R. J. *Angew. Chem., Int. Ed.* **1999**, *38*, 1813.
(36) Zhang, D.; Ma, B.; Jin, T.; Gao, S.; Yan, C.; Mak, T. C. W. *New J. Chem.* **2000**, *24*, 61.
(37) Wang, R.; Carducci, M. D.; Zheng. Z. *Inorg. Chem.* **2000**, *39*, 1836.
(38) Xu, G.; Wang, Z. M.; He, Z.; Lu, Z.; Liao, C. S.; Yan, C. H. *Inorg. Chem.* **2002**, *41*, 6802.
(39) Zhang, M.; Zhang, J.; Zheng, S.; Yang, G. *Angew. Chem., Int. Ed.* **2005**, *44*, 1385.
(40) Mudring, A.; Babai, A. *Z. Anorg. Allg. Chem.* **2005**, *631*, 261.
(41) Helgesson, G.; Jagner, S.; Poncelet, O.; Hubert-Pfalzgraf, L. G. *Polyhedron* **1991**, *13*, 1559.
(42) Evans, W. J.; Greci, M. A.; Ziller, J. W. *Inorg. Chem.* **2000**, *39*, 3213.
(43) Kritikos, M.; Moustiakimov, M.; Wijk, M.; Westin, G. *J. Chem. Soc., Dalton Trans.* **2001**, 1931.
(44) Westin, G.; Moustiakimov, M.; Kritikos, M. *Inorg. Chem.* **2002**, *41*, 3249.
(45) Moustiakimov, M.; Kritikos, M.; Westin, G. *Inorg. Chem.* **2005**, *44*, 1499.
(46) Daniele, S.; Hubert-Pfalzgraf, L. G.; Hitchcock, P. B.; Lappert, M. F. *Inorg. Chem. Commun.* **2000**, *3*, 218.
(47) Lam, A. W.; Wong, W.; Wen, G.; Zhang, X.; Gao, S. *New J. Chem.* **2001**, *25*, 531.
(48) Aspinall, H. C.; Tillotson, M. R. *Inorg. Chem.* **1996**, *35*, 2163.
(49) Li, H.; Cheng, M.; Ren, Z.; Zhang, W.; Lang, J.; Shen, Q. *Inorg. Chem.* **2006**, *45*, 1885.
(50) Hubert-Pfalzgraf, L. G.; Miele-Pajot, N.; Papiernik, R.; Vaissermann, J. *J. Chem. Soc., Dalton Trans.* **1999**, 4127.
(51) Ma, B.; Gao, S.; Bai, O.; Sun, H.; Xu, G. *J. Chem. Soc., Dalton Trans.* **2000**, 1003.
(52) Tasiopoulos, A. J.; O'Brien, T.; Abboud, K. A.; Christou, G. *Angew. Chem., Int. Ed.* **2004**, *43*, 345.
(53) Schuetz, S. A.; Silvernail, C. M.; Incarvito, C. D.; Rheingold, A. L.; Clark, J. L.; Day, V. W.; Belot, J. A. *Inorg. Chem.* **2004**, *43*, 6203.
(54) Wang, R.; Selby, H. D.; Liu, H.; Carducci, M. D.; Jin, T.; Zheng, Z.; Anthis, J. W.; Staples, R. J. *Inorg. Chem.* **2002**, *41*, 278.
(55) Sheng, J. Z.; Wen, G. J.; Cheng, W.; Yu, H. J.; Qi, S. *Jiegou Huaxue* **1990**, *9*, 140.
(56) Zhu, J. J.; Cheng, W. G.; Sheng, J. Z.; Qi, C. W. *Jiegou Huaxue* **1992**, *11*, 369.
(57) Boeyens, J. C. A.; de Villiers, J. P. R. *J. Cryst. Mol. Struct.* **1972**, *2*, 197.
(58) Zi, G.; Yang, Q.; Mak, T. C. W.; Xie, Z. *Organometallics* **2001**, *20*, 2359.
(59) Hubert-Pfalzgraf, L. G.; Daniele, S.; Bennaceur, A.; Daran, J. C.; Vaissermann, J. *Polyhedron* **1997**, *16*, 1223.
(60) Wen, G. J.; Qi, S.; Yu, H. J.; Hua, L. Y. *Jiegou Huaxue* **1990**, *9*, 184.
(61) Gao, L. X.; Zhi, L. J.; Chen, J. S.; Hua, L. Y.; Zhi, L. G. *Jiegou Huaxue* **1991**, *10*, 60.
(62) Sirio, C.; Hubert-Pfalzgraf, L. G.; Bois, C. *Polyhedron* **1997**, *16*, 1129.
(63) Freckmann, D. M. M.; Dube, T.; Berube, C. D.; Gambarotta, S.; Yap, G. P. A. *Organometallics* **2002**, *21*, 1240.
(64) Igonin, V. A.; Lindeman, S. V.; Struchkov, Y. T.; Molodtsova, Y. A.; Pozdnyakova, Y. A.; Shchegolikhina, O. I.; Zhdanov, A. A. *Izv. Akad. Nauk SSR Ser. Khim.* **1993**, 193.

## Experimental Section

**General Methods.** All syntheses were carried out under high purity nitrogen (WELCO Praxair), using conventional drybox or Schlenk techniques. Solvents (Aldrich) were purified with a dual column Solv-Tek Solvent Purification System. Nd, Se, $SeO_2$, and Hg were purchased from Strem and used as received. PhSeSePh was purchased from Aldrich and recrystallized from hexane. Melting points were taken in sealed capillaries and are uncorrected. IR spectra were taken on a Thermo Nicolet Avatar 360 FTIR spectrometer and recorded from 4000 to 600 cm$^{-1}$ as a Nujol mull on NaCl plates. Electronic spectra were recorded on a Varian DMS 100S spectrometer with the samples in a 0.10 mm quartz cell attached to a Teflon stopcock. Elemental analyses were performed by Quantitative Technologies, Inc. (Whitehouse Station, NJ). The compounds are air-sensitive and are unstable with respect to loss of lattice solvent when isolated from the mother liquor. Calculated values for the compound without lattice pyridine molecules are included in parentheses. Unit cell determinations on single crystals were obtained each time an emission measurement sample was prepared.

**Synthesis of [(py)$_{18}$Nd$_{12}$O$_6$Se$_4$(Se$_2$)$_4$(SePh)$_4$(Se$_2$Ph)$_2$Hg$_2$(SePh)$_4$]-[(Hg(SePh)$_3$]$_2$·2.8(py)(Nd12).** Nd (2.0 mmol, 0.29 g), PhSeSePh (3.0 mmol, 0.94 g), and Hg (0.30 mmol, 0.06 g) were added together in pyridine (40 mL) in a Schlenk flask under nitrogen and stirred until all the metal dissolved (24 h) to give a dark forest green colored solution. Elemental Se (2.00 mmol, 0.158 g) and $SeO_2$ (1.00 mmol, 0.111 g) were added, and the color of the reaction mixture changed to greenish black within 3 h and finally red-brown upon stirring overnight. The solution was filtered, reduced in volume to ca. 25 mL, and layered with 10 mL of hexane to give tiny yellow block-shaped crystals (0.44 g, 34%) that do not melt but turn dark red-orange at 236 °C. Anal. Calcd for C$_{200}$H$_{184}$Hg$_4$N$_{20.8}$O$_6$Se$_{30}$Nd$_{12}$: C, 30.5(29.2); H, 2.34(2.22); N 3.69(3.29). Found: C, 30.9; H, 2.63; N 3.07. UV−vis: The compound did not exhibit well-defined electronic transitions resulting from either promotion to the $\sigma$* orbital in SeSe or from any Se-to-Hg charge-transfer excitations between 300 and 750 nm, when dissolved in pyridine. IR: 2923 (m), 2854 (w), 1592 (s), 1569 (m), 1463 (s), 1378 (s), 1258 (w), 1221 (m), 1216 (s), 1144 (m), 1066 (s), 1032 (s), 1005 (m), 735 (w), 700 (w), 620 (w) cm$^{-1}$.

**X-ray Structure Determination.** Data for Nd12 were collected on a Bruker Smart APEX CCD diffractometer with graphite monochromatized Mo Kα radiation ($\lambda$ = 0.710 73 Å) at 100 K. Crystals were immersed in Paratone oil and examined at low temperatures. The data were corrected for Lorenz effects, polarization, and absorption, the latter by a multiscan (SADABS)[42] method. The structure was solved by direct methods (SHELXS86).[43] All non-hydrogen atoms were refined (SHELXL97)[44] based upon $F_{obsd}^2$. All hydrogen atom coordinates were calculated with idealized geometries (SHELXL97). Scattering factors ($f_o$, $f'$, $f''$) are as described in SHELXL97. Crystallographic data and final $R$ indices for Nd12 are given in Table 1. An ORTEP diagram[45,46] for the Nd12 core is shown in Figure 1. Significant bond geometries are given in Table 2. Complete crystallographic details are given in the Supporting Information.

**Optical Characterization.** Absorption measurements were made from THF (0.05 mM) solutions prepared by dissolving crystalline material, using a double beam spectrophotometer (Perkin-Elmer Lambda 9, Wellesley, MA) in a 1 cm cuvette using THF as the reference solvent. The emission spectra of the powdered samples were recorded by exciting the sample with a 800 nm band of a Ti sapphire ring laser (Coherent Inc, Santa Clara, CA) in the 90°-excitation geometry. The emission from the sample was focused onto a 0.55 m monochromator (Jobin Yvon, Triax 550, Edison, NJ) and detected by a thermoelectrically cooled InGaAs detector. The signal was intensified with a lock-in amplifier (SR 850 DSP, Stanford Research System, Sunnyvale, CA) and processed with a computer controlled by the Spectramax commercial software (GRAMS 32, Galactic Corp, Salem, New Hampshire). To measure the decay time, the laser beam was modulated by a chopper

**Table 1.** Summary of Crystallographic Details[a] for Nd12

| empirical formula | $C_{200}H_{184}Hg_4N_{20.8}Nd_{12}O_6Se_{30}$ |
|---|---|
| fw | 7876.92 |
| space group | $P\bar{1}$ |
| $a$ (Å) | 16.8241(12) |
| $b$ (Å) | 17.8745(12) |
| $c$ (Å) | 20.1482(14) |
| $\alpha$ (deg) | 95.650(1) |
| $\beta$ (deg) | 93.092(1) |
| $\gamma$ (deg) | 97.816(1) |
| $V$ (Å³) | 5959.6(7) |
| $Z$ | 1 |
| $D$(calcd) (g/cm⁻³) | 2.195 |
| temperature (°C) | −173 |
| $\lambda$ (Å) | 0.710 73 |
| abs coeff (mm⁻¹) | 9.758 |
| $R(F)^b$ [$I > 2\,\sigma(I)$] | 0.0655 |
| $R_w(F^2)^b$ [$I > 2\sigma(I)$] | 0.1746 |

[a] Additional crystallographic details are given in the Supporting Information. [b] Definitions: $R(F) = \Sigma||F_o| - |F_c||/\Sigma|F_o|$; $R_w(F^2) = \{\Sigma[w(F_o{}^2 - F_c{}^2)^2]/\Sigma[w(F_o{}^2)^2]\}^{1/2}$.
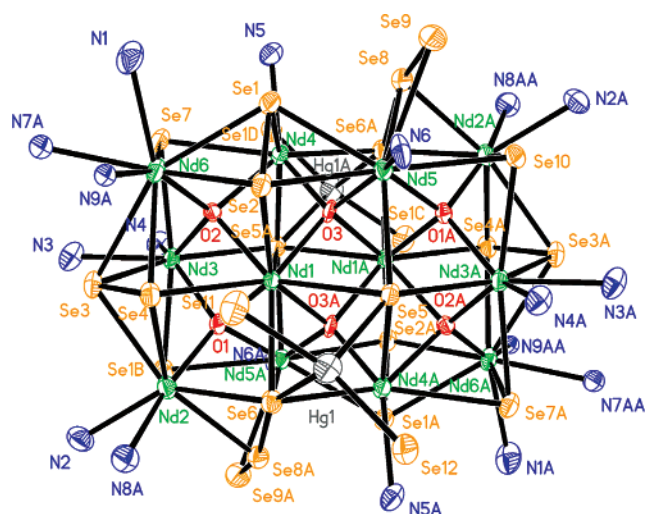


**Figure 1.** ORTEP diagram of the core atoms of the dication in Nd12, with the C and H atoms removed for clarity. Phenyl substituents are bound to Se7, Se9, and Se10.

and the signal was collected on a digital oscilloscope (model 54520A, 500 MHz, Hewlett-Packard, Palo Alto, CA).
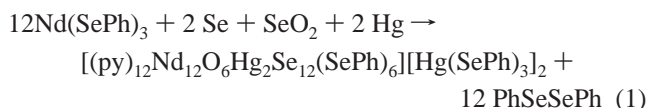
## Results

In situ prepared $Nd(SePh)_3$ reduces $SeO_2$ and Se in pyridine to form an oxo cluster (Reaction 1) that crystallizes in 30−40% yield. Low-temperature structural characterization of the product identified the compound as $[(py)_{12}Nd_{12}O_6Hg_2Se_{12}$-$(SePh)_6][Hg(SePh)_3]_2$ (Nd12). Figure 1 shows an ORTEP diagram of the Nd12 dication, and Table 2 gives a list of significant bond geometries. The structure consists of a $Nd_{12}O_6$ core, with four sets of three Nd atoms separated by pairs of tetrahedral oxo ligands, with the surface of the oxo core encapsulated with Se, SeSe, SePh, and HgSePh groups. It is a distinctly asymmetric cluster compound, with six crystallographically inequivalent Nd coordination environments that differ either by coordination number, i.e., CN = 8, Nd(1) through Nd(4); CN = 9, Nd(5) and Nd(6), or by identity of the donor atoms within the primary coordination spheres. Of the three unique Nd atoms in the internal portion of the cluster, namely Nd(1), Nd(5), and Nd(6), two are distinctive in their high coordination numbers (Nd 5, 6), while the third, Nd(1), is

**Table 2.** Significant Bond Lengths [Å] for Nd12

| | | | |
|---|---|---|---|
| Nd(1)−O(3) | 2.345(9) | Nd(1)−O(1) | 2.369(9) |
| Nd(1)−O(3)′ | 2.376(9) | Nd(1)−O(2) | 2.425(9) |
| Nd(1)−Se(6) | 3.0795(17) | Nd(1)−Se(2) | 3.1406(16) |
| Nd(1)−Se(4) | 3.2092(16) | Nd(1)−Se(5) | 3.2523(15) |
| Nd(1)−Se(5)′ | 3.9552(16) | Nd(2)−O(1) | 2.256(10) |
| Nd(2)−Se(8)′ | 2.9956(17) | Nd(2)−Se(6) | 3.0032(16) |
| Nd(2)−Se(4) | 3.0107(17) | Nd(2)−Se(3) | 3.0932(18) |
| Nd(2)−Se(10)′ | 3.1030(17) | Nd(3)−O(1) | 2.345(9) |
| Nd(3)−O(2) | 2.365(9) | Nd(3)−Se(5)′ | 2.9779(16) |
| Nd(3)−Se(3) | 3.0385(18) | Nd(3)−Se(10)′ | 3.0577(17) |
| Nd(3)−Se(7) | 3.0658(17) | Nd(4)−O(3) | 2.244(9) |
| Nd(4)−O(2) | 2.449(9) | Nd(4)−Se(5)′ | 3.0212(16) |
| Nd(4)−Se(6)′ | 3.0413(16) | Nd(4)−Se(1) | 3.0679(17) |
| Nd(4)−Se(7) | 3.1224(16) | Nd(4)−Se(8) | 3.6837(17) |
| Nd(5)−O(3) | 2.287(9) | Nd(5)−O(1)′ | 2.426(9) |
| Nd(5)−Se(5) | 3.0433(17) | Nd(5)−Se(8) | 3.0532(18) |
| Nd(5)−Se(1) | 3.1213(16) | Nd(5)−Se(10) | 3.1270(16) |
| Nd(5)−Se(2) | 3.1817(16) | Nd(5)−Se(9) | 3.3157(19) |
| Nd(6)−O(2) | 2.256(9) | Nd(6)−Se(2) | 3.0034(16) |
| Nd(6)−Se(4) | 3.0582(18) | Nd(6)−Se(1) | 3.1631(17) |
| Nd(6)−Se(7) | 3.1743(18) | Nd(6)−Se(3) | 3.2994(18) |
| O(1)−Nd(5)′ | 2.426(9) | O(3)−Nd(1)′ | 2.376(9) |
| Se(1)−Se(2) | 2.392(2) | Se(3)−Se(4) | 2.365(2) |
| Se(5)−Nd(3)′ | 2.9779(16) | Se(5)−Nd(4)′ | 3.0212(16) |
| Se(6)−Nd(4)′ | 3.0413(16) | Se(7)−C(1) | 1.924(15) |
| Se(8)−Se(9) | 2.429(2) | Se(8)−Se(6)′ | 2.910(2) |

the only Nd in the structure that does not coordinate to a neutral pyridine donor. Nd(1) is also the only Nd to coordinate to more than two oxo ligands, with direct bonds to O(1), O(2), O(3), and O(3)′. The terminal cluster regions are bound to a greater number of pyridine ligands, presumably because they are unconstrained by the presence of the two $Hg(SePh)_2$ moieties that are covalently bound to the Se in the cluster surface.

$$12 Nd(SePh)_3 + 2\,Se + SeO_2 + 2\,Hg \rightarrow$$
$$[(py)_{12}Nd_{12}O_6Hg_2Se_{12}(SePh)_6][Hg(SePh)_3]_2 +$$
$$12\,PhSeSePh \quad (1)$$

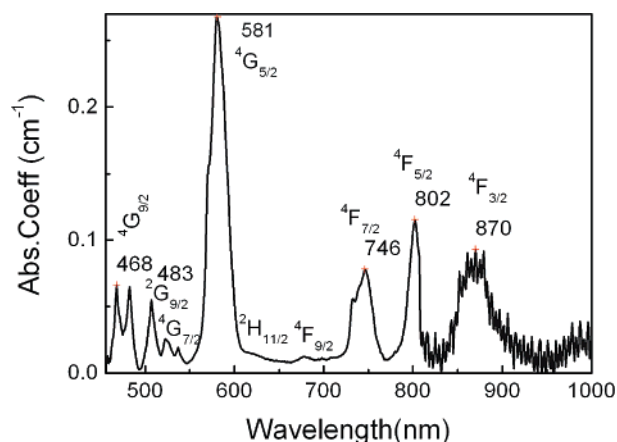The absorption spectrum of Nd12 is shown in Figure 2 and



**Figure 2.** Absorption spectrum of Nd12 measured in THF with a concentration of 0.05 mmol.

is similar to $Nd^{3+}$ spectral transitions of typical solid-state materials with comparable absorption coefficients.[70−73] The emission spectrum, obtained by exciting the metastable level $^4F_{3/2}$, is shown in Figure 3. Three well resolved emission bands are observed at 926, 1082, and 1352 nm corresponding to the transitions from $^4F_{3/2}$ to $^4I_{9/2}$, $^4I_{11/2}$, and $^4I_{13/2}$ levels. In order to
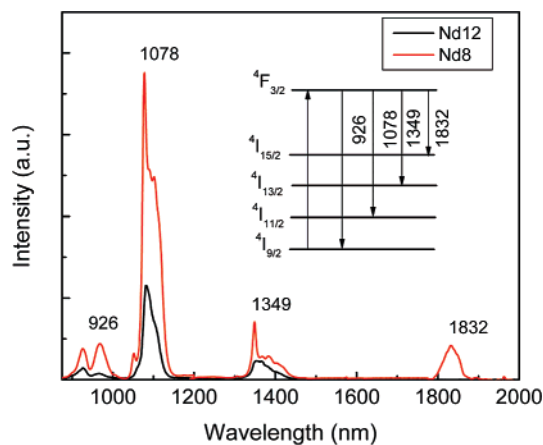
**Figure 3.** Emission spectrum of Nd12 (black) and Nd8 (red) obtained by excitation at the $^4F_{3/2}$ band by the 800 nm emission of a Ti Sapphire laser. The band positions for Nd12 [926, 1082, and 1352 nm] and Nd8 [926, 1078, and 1349 nm] are for the emission transitions from $^4F_{3/2}$ to $^4I_{9/2}$, $^4I_{11/2}$, and $^4I_{13/2}$ levels, respectively. Solid-state $Nd_2O_3$ does not emit at either 1349 or 1832 nm.

measure the quantum efficiency of the $^4F_{3/2} \rightarrow {}^4I_{11/2}$ transition, the fluorescence decay time ($\tau_{fl}$) was extracted from the measured decay curve shown in the Supporting Information. The decay curve was fitted with the Monte Carlo model[74] to yield a decay time of 141 $\mu$s for the 1082 nm emission. The fitting takes into account all the cooperative energy transfer processes between Nd atoms located in the various crystallographic sites. The effective experimental decay time, together with the calculated radiative decay time[75,76] of 1160 $\mu$s results in a calculated quantum efficiency of 12% for Nd12.

## Discussion

Chalcogen encapsulation of high nuclearity oxo clusters appears to be an effective method for inhibiting disproportion-ation and the deposition of solid-state oxides, as was initially proposed in the synthesis of the relatively small octanuclear clusters $(THF)_8Ln_8O_2Se_2(SePh)_{16}$ (Ln = Ce, Pr, Nd, Sm).[21] The Nd12 product reported here has a considerably larger percentage of oxo ligands, with a structurally diverse set of selenium based anions surrounding the oxo core. These clusters appear to be stable with respect to ligand redistribution reactions and the precipitation of $Nd_2O_3$. It should be noted that, in the thermolysis of $(THF)_8Nd_9O_2Se_2(SePh)_{16}$, disproportionation to give $LnO_x$

(65) Bruker-ASX. SADABS, Bruker Nonius area detector scaling and absorption correction, v2.05, Bruker-AXS Inc., Madison, Wisconsin, 2003.
(66) Sheldrick, G. M. SHELXS86, Program for the Solution of Crystal Structures, University of Göttingen, Germany, 1986.
(67) Sheldrick, G. M. SHELXL97, Program for Crystal Structure Refinement, University of Göttingen, Germany, 1997.
(68) Johnson, C. K. ORTEP II, Report ORNL-5138. Oak Ridge National Laboratory, Oak Ridge, TN, U.S.A., 1976.
(69) Sheldrick, G. M. SHELXTL (XP). Version 6.14. Bruker-AXS, Inc., Madison, Wisconsin, U.S.A., 2000.
(70) Oczko, G. *J. Alloys Compd.* **2000**, *300*, 414.
(71) Lis, S. *J. Alloys Compd.* **2000**, *300*, 88.
(72) Gubina, K. E; Shatrava, J. A.; Ovchynnikov, V. A.; Amirkhnov, V. M. *Polyhedron* **2000**, *19*, 2203.
(73) Legendziewicz, J.; Oczko, G.; Wiglusz, R.; Amirkhanov, V. *J. Alloys Compd.* **2001**, *323*, 792.
(74) Díaz Torres, L. A.; Barbosa-Garcia, O.; Meneses-Nava, M. A. Struck, C. W.; Di Bartolo, B. In *Advances in Energy Transfer Processes*; Di Bartolo, B., Chen, X., Eds.; World Scientific Publishing Co.: Singapore, 2000; pp 523−552.
(75) (a) Judd, B. R. *Phys. Rev. B* **1962**, *127*, 750. (b) Ofelt, G. S. *J. Chem. Phys.* **1962**, *37*, 511.
(76) Kaminskii, A. A. *Laser Crystals, Their Physics and Properties*; Springer-Verlag: Berlin, 1981.

and $LnSe_x$ was observed, and the present cluster can be viewed as an intermediate along this molecules-to-solids pathway.

The molecular structure of the $(py)_{12}Nd_{12}Hg_2Se_{12}(SePh)_6$ dication is composed of a $Nd_{12}O_6$ kernel surrounded by Se, $Se_2$, and $Se_2Ph$ bridging ligands and capped by SePh, py, and Hg-$(SePh)_2$ groups. While this Nd12 cluster is by far the most complicated lanthanide oxo cluster reported to date, there are a significant number of simpler compounds available for comparison. For $Ln_4O$ containing structures in the Cambridge Structural Database,[77] the O atom generally resides in one of four sites: (A) the center of a $Ln_4$ tetrahedron,[28−29,46,55−61] as is the case in the structure presented here, where the extended $Nd_{12}O_6$ core region contains six examples of O atoms very close to their respective tetrahedron centroid (O...$Ln_4$−centroid < 0.25 Å); (B) off-center of the $Ln_4$ tetrahedron,[30,32,62] such that there is an opening of one edge of the $Ln_4$ tetrahedron and one Ln−O−Ln angle is near 180° (0.5 Å < O...$Ln_4$-centroid <0.8 Å);[47,63−64] (C) at the center of a square-planar arrangement of the $Ln_4$ (O...$Ln_4$−centroid ∼0 Å); and (D) capping a square-planar $Ln_4$ face (0.5 Å < O...$Ln_4$−centroid < 0.8 Å).[42]

In addition to four coordinate Ln−oxo structures, there exist an extraordinary range of additional oxo geometries, from the linear or slightly bent Ln−O−Ln found in numerous bimetallic molecules,[22−26] to trigonal planar, pentagonal bipyramidal, and octahedral bonding environments. A coordination number of 2 results when the ancillary ligands inhibit ligand redistribution processes, i.e., in the $[Cp^*_2Ln]_2O$ compounds, where dispro-portionation to give $Cp^*_3Ln/[Cp^*LnO]$ is energetically unfavor-able because of the ligand−ligand repulsions in $Cp^*_3Ln$. Smaller ancillary ligands do not prevent redistribution, and so oxo geometries with higher coordination numbers (and the associated increase in nuclearity) become possible. The present cluster contains a varied array of weakly bound chalcogen encapsulants and flexible monodentate pyridine donor ligands that comprise a particularly pliable set of ancillary ligands. The shallow potential energy surfaces that define Ln−Se and Ln−N(py) interactions are clearly secondary in importance to the optimiza-tion of Ln−O bonding interactions, and the result is a diverse ancillary ligand system that facilitates adoption of the tetrahedral oxo geometry. The absence of any octahedral oxo ligand environment can also be understood by noting that in the solid-state oxide there is no alternative for increasing Ln coordination numbers, whereas in the present compound there is an abun-dance of ancillary anions with well delocalized charges available to saturate the assortment of Nd coordination environments.

The extended $Nd_xO_y$ core region of the $Nd_{12}$ dication affords, for the first time, the comparison of the internal $Ln_xO_y$ core of a predominantly organic molecule with the inorganic structure of its pyrolytic product, $Ln_2O_3$. Figure 4 illustrates the similari-ties of the two cores, with the organic fragments of the cluster removed for clarity. In the solid-state structure of $Nd_2O_3$,[78] although all of the Nd atoms are seven-coordinate with a single characteristic environment, the O atoms have two types of environments, namely, tetrahedral two-thirds of the time and octahedral one-third of the time (giving the $Nd/O_t/O_o$ ratio 2:2:1 for overall stoichiometry $Nd_2O_3$). In the $Nd_{12}$ cation, all of the

(77) Allen, F. H.; Bellard, S.; Brice, M. D.; Cartwright, B. A.; Doubleday, A.; Higgs, H.; Hummelink, T.; Hummelink-Peters, B. G.; Kennard, O.; Motherwell, W. D. S.; Rodgers, J. R.; Watson, D. G. *Acta Crystallogr.* **1979**, *B35*, 2331.
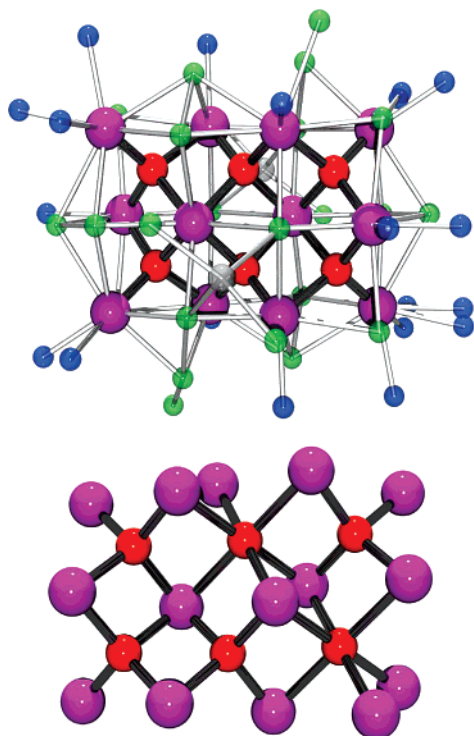(78) Boucherle, J. X.; Schweizer, J. *Acta Crystallogr.* **1975**, *B31*, 2745.

**Figure 4.** Representation of the $Nd_{12}O_6$ core and a fragment of the $Nd_2O_3$ lattice, with purple Nd and red O.

O atoms are tetrahedral, bonded to Nd only, and form only a single $O_6$ layer, rather than the extended $O_\infty$ of the $Nd_2O_3$ coordination compound. The Nd–O bond lengths in $Nd_2O_3$ are three at 2.30 Å ($O_t$), one at 2.40 Å ($O_t$), and three at 2.66 Å ($O_h$). The shorter (tetrahedral) of these compare well to those in the Nd12 dication, which range from 2.24 to 2.45 Å, where the bond-elongating Nd–O bond strain for the octahedral situation in $Nd_2O_3$ is absent. The average Nd–O bond length for the tetrahedral oxygen in Nd12 and $Nd_2O_3$ are 2.34 and 2.33 Å, respectively.

The Nd12 structure is not general for other Ln, with identical experiments using Pr or Sm yielding no crystalline products. Whether this specificity is or is not going to be noted frequently in the synthesis of larger Ln clusters remains to be seen. A general isolability was noted for octanuclear (solvent)$_8Ln_8E_6$-$(EPh)_{12}$ (E = S, Se) clusters[79−82] spanning most of the Ln series La−Er, but only three Ln gave the decanuclear clusters $(THF)_xLn_{10}S_6(SeSe)_6I_6$ products (Ln = Ho, Er, Tm).[83] It is reasonable to assume that multiplying the effect of single Ln ionic radii changes by *n* in an *n* atom cluster is going to impact upon the ability of surface ligands to effectively saturate the cluster perimeter. With Ln coordination geometries defined by such shallow energy potentials, changes in the Ln ionic radius could easily lead to distortions in the cluster surface, particularly when, as in this case, there is a variety of ancillary ligands available.

The present cluster has hybrid electronic properties that blend the characteristics of molecular and solid-state compounds, with

a quantum efficiency of 12% and measurable emission at 1.34 $\mu$m. Earlier we reported efficiencies of the order of 16% for $(DME)_2Nd(SC_6F_5)_3$ and $(THF)_8Nd_8O_2Se_2(SePh)_{16}$ that were, and still are, the highest reported efficiencies for emission from molecular Nd compounds.[21] For comparison, Hasegawa et al. have obtained a decay time of 13 $\mu$s and a quantum efficiency of 3.2% in Nd (bis-perfluorooctanesulfonylimide)$_3$,[84] and in all other reports[85−90] the quantum efficiencies obtained are in the range 0.001−1.0%. The present example, while not as luminous on a per Nd basis, is capable of delivering higher concentrations of Nd into organic matrices.

The low-energy emissions are particularly important properties of these compounds, with the two lowest energy transition emissions falling within the range that would be useful in the telecommunications industry. Significantly, Nd12 emits 1352 nm radiation, as was noted in the emission spectra of the Nd thiolate and Nd8 cluster mentioned above. This 1352 nm emission is absent in measurements recorded on solid-state $Nd_2O_3$. In contrast, Nd12 is similar to $Nd_2O_3$ in that it does not emit at 1832 nm. This particularly low-energy emission was observed in the spectra of $(DME)_2Nd(SC_6F_5)_3$ and $(THF)_8$-$Nd_8O_2Se_2(SePh)_{16}$.

The disappearance of the 1832 nm emission band in Nd12 can be explained in terms of vibronic behavior within the structure of the Nd12 complex. The Nd12 compound has a core consisting of continuous $Nd_3O_2$ layers, with the tetrahedral oxo ligand essentially identical to those found in $Nd_2O_3$.[78] This $Nd_2O_3$-like core structure facilitates a higher multiphonon relaxation rate, as is typically seen in high phonon energy hosts. As seen from Figure 5, this multiphonon relaxation drastically quenches the emission of the $^4F_{3/2} \rightarrow {}^4I_{15/2}$ transition. In $Nd_2O_3$ the oxygen atom is tetragonally coordinated with $Nd^{3+}$, and this leads to a high phonon energy environment with a frequency on the order of 1200 cm$^{-1}$ that is sufficient to quench most of the emissions, especially the 1832 nm band.

The quantum efficiency of the present Nd12, being greater than solid-state $Nd_2O_3$ but less than $Nd(SC_6F_5)_3$ or the Nd8 cluster, can be understood in terms of the coordination environments of the Nd atoms in the cluster. From the molecular structure, it is clear that the Nd ions are mostly bound to Se based anions; of the 100 bonds to Nd in the structure, only 24 are bonds to oxo ligands, 9 are to pyridine nitrogen, and the remaining 58 bonds involve some form of interaction with the Se electron density. As reported in our earlier Nd complexes this heavy anion coordination provides a low phonon energy environment for the molecular cluster, and that results in intense infrared emission. With a low vibrational frequency of the host, multiphonon relaxation losses diminish, and more intense infrared emission can be expected. A comparison of the

(79) Freedman, D.; Emge, T. J.; Brennan, J. G. *J. Am. Chem. Soc.* **1997**, *119*, 11112.
(80) Melman, J. H.; Emge, T. J.; Brennan, J. G. *Chem. Commun.* **1997**, 2269.
(81) Melman, J. H.; Emge, T. J.; Brennan, J. G. *Inorg. Chem.* **1999**, *38*, 2117.
(82) Freedman, D.; Emge, T. J.; Brennan, J. G. *Inorg. Chem.* **1999**, *38*, 4400.
(83) Huebner, L.; Kornienko, A.; Emge, T. J.; Brennan, J. G. *Inorg. Chem.* **2005**, *44*, 5118.

(84) Hasegawa, Y.; Ohkubo, T.; Sogabe, K.; Kawamura, Y.; Wada, Y.; Nakashima, N.; Yanagida, S. *Angew. Chem., Int. Ed.* **2000**, *39*, 357.
(85) Wolbers, M. P. O.; van Veggel, F. C. J. M.; Hofstraat, J. W.; Geurts, F. A. J.; Reinhoudt. D. N. *J. Chem. Soc., Perkin Trans.* **1997**, 2275.
(86) Wolbers, M. P. O.; van Veggel, F. C. J. M.; Snellink-Ruel, B. H. M.; Hofstraat, J. W.; Geurts, F. A. J.; Reinhoudt, D. N. *J. Chem. Soc., Perkin Trans.* **1998**, 2141.
(87) Klink, S. I.; Hebbink, G. A.; Grave, L.; van Veggel, F. C. J. M.; Reinhoudt, D. N.; Slooff, L. H.; Polman, A.; Hofstraat, J. W. *J. Appl. Phys.* **1999**, *86*, 1181.
(88) Hebbink, G. A.; van Veggel, F. C. J. M.; Reinhoudt, D. N. *Eur. J. Org. Chem.* **2001**, 4101.
(89) Hasegawa, Y.; Murakoshi, K.; Wada, Y.; Kim, J. H.; Nakashima, N.; Yamanaka, T.; Yanagida, S. *Chem. Phys. Lett.* **1996**, *248*, 8.
(90) Wada, Y.; Okubo, T.; Ryo, M.; Nakazawa, T.; Hasegawa, Y.; Yanagida, S. *J. Am. Chem. Soc.* **2000**, *122*, 8583.
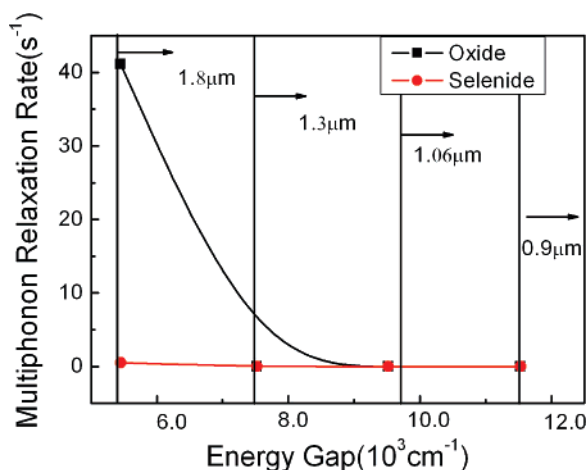
**Figure 5.** Comparison of the effect of multiphonon relaxation on the observed fluorescence bands of $Nd^{3+}$ in selenide and oxide hosts. The almost straight-line behavior shows that multiphonon relaxation is almost independent of the emission process in Nd doped selenides. In oxides the effect is more prominent for the 1832 nm emission and goes off exponentially with the energy gap.

influence of the multiphonon relaxation in a chalcogenide and an oxide host on the four emission bands in $Nd^{3+}$ is shown in Figure 5. This figure shows that in a low phonon energy host like Nd12 the infrared emission is independent of the multiphonon relaxation, whereas in a high phonon energy host like $Nd_2O_3$ vibrational relaxation is the major parameter controlling the infrared emission characteristics. The relative decrease in quantum efficiency of Nd12 compared with the previously reported Nd8 is also consistent with the increasing number of high phonon energy Nd−O ligands in the former.

In addition to lattice phonons, vibrations in C−H functional groups are potential quenchers of $Nd^{3+}$ emission. The $^4F_{3/2} \rightarrow {}^4I_{15/2}$ energy gap matches with the vibration modes of CH (2950 $cm^{-1}$) and hence can contribute to the efficient nonradiative deactivation of the $^4F_{3/2}$ level. The quenching due to overtones of the CH bands originating with the pyridine and Ph(Se) ligands encapsulating the cluster core is prominent for the $^4F_{3/2} \rightarrow {}^4I_{15/2}$, $^4I_{11/2}$, and $^4I_{9/2}$ emission bands. Both py and SePh are weakly bound to Nd, relative to the oxo and selenido dianions, and the Ph groups are distanced significantly from Nd by relatively long Nd−Se bond lengths. Nevertheless, it seems reasonable to assume that the multitude of C−H bonds have also detracted from optimal quantum efficiency. Elimination of SePh ligands will presumably improve quantum efficiency.

One final factor influencing quantum efficiency is concentration quenching or Ln−Ln relaxation. Generally, in solid-state materials QE can be optimized by controlling the proximity of nearest neighbor Ln.[91] Emissive Ln materials usually contain the desired Ln ion doped into an inert matrix, i.e., Nd doped

La solids.[76] In the series $Nd(SC_6F_5)_3$, Nd8, and Nd12, there are increasing numbers of Ln−Ln interactions that can lead to a decrease in emission intensity. More significantly, the Ln−Ln separations decrease as the bridging chalcogen anions are replaced by smaller oxo ligands. Our detailed energy transfer calculations[92] show that in Nd12 the energy transfer is through a combination of supermigration and dipole−dipole interactions. Within the Nd12 complex each Nd ion has at least one first neighbor at a separation of less than 0.39 nm. The average number of first neighbors in the inner core is 2.6 Nd for separation distances smaller than 0.39 nm. As such, all Nd ions can have fast energy transfers to nearest neighbors, driven by single dipole−dipole interactions. As a consequence, at short times energy transfer to first neighbors is always present, and all the unexcited Nd ions will act as trap centers to quench the luminescence of the $^4F_{3/2}$ state by a dipole−dipole driven migration energy transfer process. Results of the simulations yield a critical separation of 0.64 nm in Nd12. In Nd12 the shortest separation between Nd ions is 0.37 nm, whereas the longest is 1.03 nm. Since the shortest separation between two interacting $Nd^{3+}$ ions is less than the critical separation, Nd12 has efficient quenching of the excited Nd ions by energy transfer to the first neighboring Nd ions. Also, since the average number of first neighbors for each excited Nd in Nd12 is higher (2.6 neighbor/Nd ion) than that in either Nd8 (1.5 Neighbor/Nd ion) or the molecular thiolate, the migration process is more dominant in Nd12.

## Conclusions

Increasingly large oxo cluster compounds of the lanthanides can be prepared and stabilized with electropositive chalcogen encapsulants. With cluster dimensions greater than 1 nm, these materials exhibit hybrid molecular/solid-state properties, including structural characteristics that resemble solid-state lanthanide oxides and emission properties that blend the characteristics of molecular and solid-state sources. Both vibronic coupling and concentration quenching have a significant influence upon emission intensity.

**Supporting Information Available:** X-ray crystallographic files in CIF format for the crystal structure of Nd12. Fluorescence decay curve and exponential fit. This material is available free of charge via the Internet at http://pubs.acs.org.

JA069000A

(91) Di Bartolo, B. In *Energy Transfer Processes in Condensed Matter*; Di Bartolo, B., Ed.; Plenum Press: New York, 1984; p 103.
(92) Kumar, G. A.; Riman, R. E.; Diaz Torres, L. A.; Banerjee, S.; Emge, T. J.; Brennan, J. G. In preparation.